

Seafloor Asymmetry in the Atlantic Ocean

S.S. Gao*, K.H. Liu

Department of Geology, Kansas State University, Manhattan, KS 66506, USA

(Received June 30, 2004; accepted July 27, 2004)

Abstract Measurements of seafloor asymmetry at about 360 000 pairs of conjugate points along 1250 profiles across the mid-Atlantic Ridge (MAR) provide new constraints on models for the upwelling of the buoyant asthenosphere. The sign and amplitude of the asymmetry vary systematically and are functions of the distance between the spreading center and the location of the inferred location of maximum regional buoyancy (LMRB) in the asthenosphere. The LMRB is a smooth line derived from the observed asymmetry and is more centered at the regional topographic high than the spreading center. These observations are best explained by active upwelling of the underlying buoyant asthenosphere rather than by pressure-release melting.

Key words seafloor topography; seafloor asymmetry; mid-ocean ridges; Atlantic Ocean

Number ISSN 1672-5182(2004)02-191-04

1 Introduction

The mid-ocean ridge system is the largest geologic structure on Earth. One of the original models on ridge processes considers the upwelling of the underlying asthenosphere as the result of the active ascending of a large-scale convection cell in the mantle (Holmes, 1931; Hess, 1962), and a more recent model suggests that the upwelling is passively created by pressure-release melting of basaltic minerals (Turcotte and Schubert, 2002; Oxburgh and Parmentier, 1977). The latter implies that on a regional scale, the anomalous asthenosphere is located directly beneath the spreading center and should migrate with the center if it is displaced by a transform fault (TF). Numerous studies (Marty and Cazenave, 1989; Kane and Hayes, 1992; Calcagno and Cazenave, 1994; Forsyth *et al.*, 1998; Eberle and Forsyth, 1998; Conder *et al.*, 2002; Doglioni *et al.*, 2003), however, have found significant asymmetry in elevation, subsidence rates, or both, across oceanic and continental rifts. A number of competing models (Cochran, 1986; Marty and Cazenave, 1989; Phipps Morgan and Smith, 1992; Conder *et al.*, 2002; Doglioni *et al.*, 2003) have been proposed to explain the asymmetry. Most of those models are either based on a limited number of elevation profiles derived from low-resolution databases, or are for areas affected by particular large-scale structures such as the East Pacific Superswell.

Here we present measurements of seafloor asymmetry

along the section of the MAR between latitudes 30°N and 38°S, in which the influence of major plumes and triple junctions on seafloor topography is relatively small (Fig.1).

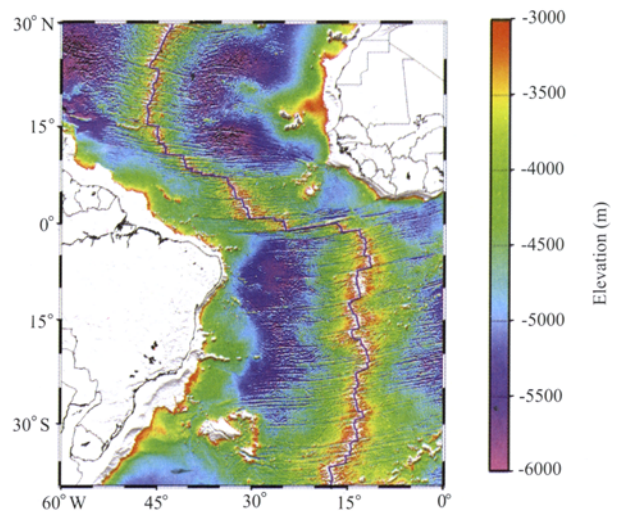


Fig.1 Seafloor bathymetry in the study area
The purple line is the spreading center.

2 Data and Methods

The 2-minute-resolution digital bathymetric data used in the study were obtained by combining ship depth soundings with marine gravity observations from spacecraft (Smith and Sandwell, 1997). In addition, we use an independent bathymetric data set, ETOPO-5 (NOAA, 1988)^①, and a database from inversion of altimetry-based mean sea surface and ship depth soundings (Calmant *et al.*, 2002) to verify the

* Corresponding author. <http://earth.geol.ksu.edu>
E-mail: gao@ksu.edu; Tel: 785-532-2243; Fax: 785-532-5159

results.

In order to measure seafloor asymmetry between the conjugate points across the mid-ocean ridge, the geographic coordinates of about 1250 points of the spreading center are determined by using a pattern-recognition program, which searches for the locations of the central valley (Fig.2). The resulting spreading center is visually checked to ensure that the program works properly. The NS distance between neighboring points is 0.05° (about 5.6 km).

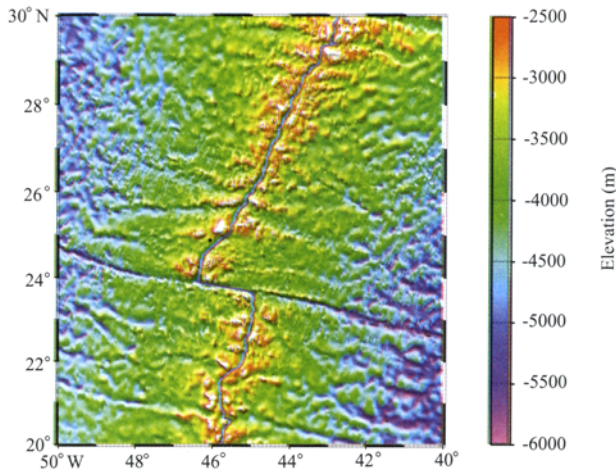


Fig.2 Resulting coordinates of the spreading center. (purple line) found by searching for the central valley using a pattern-recognition program

For the i th point on the spreading center, the geographic coordinates of evenly-spaced locations along a small circle arc extending approximately eastward and starting from the point are calculated from the rotation poles between the corresponding plates (DeMets *et al.*, 1990), and the elevation for each of the locations, h_{ij} , where j ranges from 1 to 278, is extracted from the bathymetric database (Smith and Sandwell, 1997). The distance between the neighboring locations on an arc is 4 km, and thus the total length of the arc is about 1100 km on each side of the spreading center, where the seafloor ages range from 0 to about 85 Ma (Muller *et al.*, 1997). Similarly, elevations are extracted at conjugate points along a small-circle arc extending approximately westward starting from the same point on the spreading center. The asymmetry (δh_{ij}), which is the elevation difference between the eastern and western sides, is then calculated (Fig.3 a). The averaged difference over the arcs between the eastern and western sides of the i th point on the spreading center, $\delta \bar{h}_i$, is shown in Fig.3 b.

3 Results

The results show rapid longitudinal changes of the asymmetry across most of the significant TFs and corresponding fracture zones, and relatively smooth variation within the same lithospheric blocks (Figs.3 a and 3 b). In the entire study area $\delta \bar{h}_i$ has a mean of -26

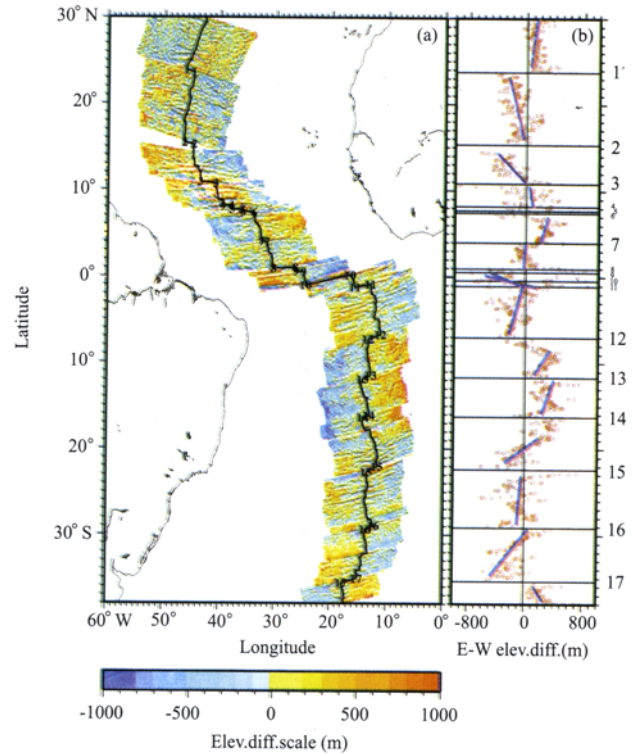


Fig.3 (a) Elevation difference between the eastern and conjugate western sides of the MAR. Numbered EW sections indicate transform faults with a displacement of 100 km or larger. (b) Mean east-west elevation differences ($\delta \bar{h}_i$) along the ridge. For the i th point on the ridge, $\delta \bar{h}_i$ is calculated using $1/278 \sum_{j=1}^{278} \delta h_{ij}$. Blue bars represent the best-fit of the measurements with small (≤ 20 m) errors for each of the blocks between adjacent TFs.

± 14 m, suggesting that overall the MAR is highly symmetric. In our study area (Fig.1) a recent study (Doglioni *et al.*, 2003) measured the asymmetry along four profiles, all of which showed that the eastern sides are higher than the conjugate western sides. This is inconsistent with our conclusions, which were drawn from measurements along 1250 profiles. Therefore, the observation that the eastern sides of the major oceanic and some continental rifts are higher than the conjugate western sides and the associated 'westward drift of the lithosphere' model (Doglioni *et al.*, 2003) are unlikely to be universally true.

Almost identical results were obtained by using the ETOPO-5 database^① and a database from inversion of altimetry-based mean sea surface and ship depth soundings (Calmant *et al.*, 2002). The correlation coefficients between $\delta \bar{h}_i$ (Fig.3 b) and corresponding measurements from the two databases are 0.948 and 0.996, respectively. Such a high level of similarity suggests that observation errors in the bathymetric database (Smith and Sandwell, 1997) used to obtain the

① National Oceanic and Atmospheric Administration (NOAA), 1988. ETOPO-5 Bathymetry/Topography Data Announcement 88-MGG-02: Digital Relief of the Surface of the Earth. Natl. Geophys. Data Cent.

results shown in Fig.3 are unlikely to have any substantial effects on the computed results.

Spatial variation in sediment thickness and associated sediment loading can bias the results. However, a recent digital sediment thickness database compiled by the U.S. National Geophysical Data Center (NGDC) indicates that in the study area the thickness of the sediments is between 0 and 150 m, which is several times smaller than most of the $\delta\bar{h}_i$ observations. In addition, in order for sediments to bias the observations, an asymmetric distribution in thickness with frequent reversal of sign across the TFs is required. Such an asymmetry is physically implausible and is not found in the NGDC database.

Another possible factor to be considered in the observations is the difference in age (t) between conjugate points. Both theoretical and observational studies suggest that seafloor depth is a linear function of \sqrt{t} if the seafloor is younger than 70–90 Ma (Marty and Cazenave, 1989; Parsons and Sclater, 1977), *i.e.*, $d(t) = 2500 + 350\sqrt{t}$, where d is seafloor depth in meters, and t is crustal age in Ma. We compute δt_{ij} , the difference in t between the conjugate points at which asymmetry in bathymetry is obtained, based on a digital isochron database (Muller *et al.*, 1997), and we find no correlation between δt_{ij} and δh_{ij} . This suggests that the asymmetry in seafloor elevation is not caused by asymmetry in spreading rate.

We speculate that the sign and the amplitude of the asymmetry are functions of the distance between the spreading center and an imaginary line (Fig.4) constructed based on the following criteria: 1) Unlike the

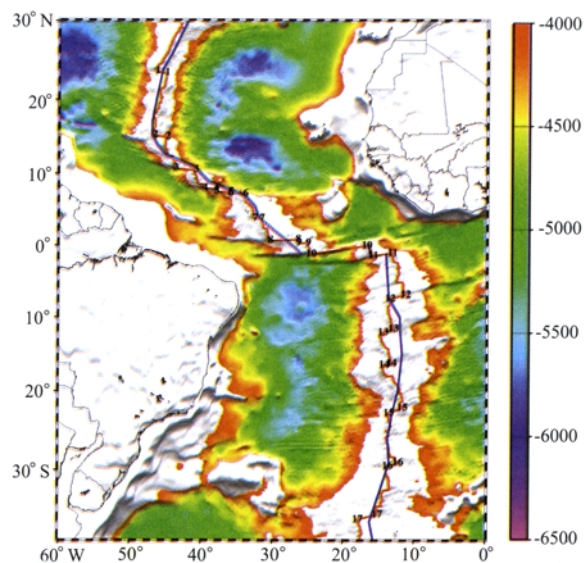


Fig.4 Seafloor topography, MAR (red line), and the predicted approximate location of maximum regional buoyancy (blue line) in the study area

The elevations are low-pass filtered using a median filter with a 50 km radius. The white areas are higher than -4000 m. Dotted blue lines represent sections of the LMRB with large uncertainties in location.

spreading center, which is frequently displaced by the TFs, the line is continuous except at the boundary between the north and south Atlantic basins; 2) it intersects with the spreading center or the transform faults at locations where the asymmetry changes sign. Therefore the side on which the line is located is on average higher than the other side, and a larger amplitude of the asymmetry is observed for a greater distance. Interestingly, the resulting line is more centered at the regional topographic high than the spreading center (Fig.4).

4 Discussion and Conclusion

The observations can be explained by a model (Fig.5) involving movement of the lithosphere relative to the

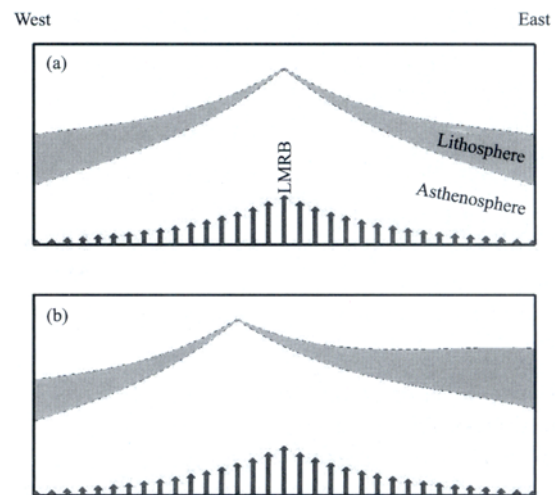


Fig.5 Schematic diagrams to explain the observations (a) The 'normal' situation under which the ridge is directly on top of the location of maximum regional buoyancy (LMRB), resulting in symmetric seafloor topography. The length of the vertical arrows schematically represents the strength of the buoyancy. (b) The lithosphere is shifted to the west relative to the LMRB, resulting in higher elevation on the eastern side.

location of maximum regional buoyancy (LMRB) in the asthenosphere, which is represented by the imaginary line shown in Fig.4. This model suggests that the LMRB is the center of a hotter and consequently lighter and actively upwelling asthenosphere, which is the ascending limb of a large-scale convection cell in the mantle (Holmes, 1931; Hess, 1962). Such an anomalous asthenosphere is evident in numerous seismic tomographic models (Grand *et al.*, 1997; King and Ritsema, 2000), which revealed a broad low-velocity zone extending to a depth of a few hundred kilometers. Our model, which involves active upwelling of the anomalous asthenosphere, predicts that relative to the spread center, the longitudinal variation of the LMRB must be smooth and is hardly affected by displacement of the lithosphere along the TFs. Low-pass filtered elevations (Fig.4) support this hypothesis. The TFs displaced a zone of about 100–200 km wide,

but it had almost no effects on regional topography beyond this zone.

This model suggests that seafloor bathymetry is determined jointly by the age-dependent subsidence of the lithosphere and the density of the asthenosphere. For a lithospheric block that is shifted westward relative to the LMRB, the eastern side is uplifted by the hotter and more buoyant asthenosphere relative to the conjugate western side, and vice versa (Fig.5). A larger distance between the spreading center and the LMRB should correspond to a larger $\delta\bar{h}_i$, although the correspondence may not necessarily be linear.

The observations imply that much of the MAR is shifted either toward the east or the west relative to the LMRB and rarely stays directly on top of it (Figs.3 and 4), suggesting possible decoupling between the lithosphere and the underlying asthenosphere. This conclusion is consistent with seismological observations such as those of shear-wave splitting (Gao *et al.*, 1994; Silver and Holt, 2002), which measures preferred orientation of anisotropic minerals in the mantle such as olivine due to mantle deformation. The observed characteristics of the asymmetry suggests that the buoyant asthenosphere is the consequence of an active upwelling process associated with the ascending limb of a large-scale convection cell in the mantle (Holmes, 1931; Hess, 1962), rather than the result of pressure-release melting of basaltic minerals. The latter process might be responsible for the formation of magma chambers which are directly beneath the spreading center and are more localized relative to the underlying broad anomalous asthenosphere. In summary, our measurements support active rather than passive upwelling of the asthenosphere beneath the MAR.

Acknowledgements

The elevation databases were provided by D. Sandwell and S. Calmant. The figures were produced by using GMT (Wessel and Smith, 1995). Discussions with G. Clark, P. Davis, M. Hubbard and C. Oviatt are greatly appreciated. This work was partially supported by the U. S. National Science Foundation under contract No.0207466.

References

- Calcagno, P., and A. Cazenave, 1994. Subsidence of the seafloor in the Atlantic and Pacific Oceans: regional and large-scale variations. *Earth Planet. Sci. Lett.*, **126**: 473–492.
- Calmant, S. C., M. Berge-Nguyen, and A. Cazenave, 2002. Global seafloor topography from a least-squares inversion of altimetry-based high-resolution mean sea surface and shipboard soundings. *Geophys. J. Int.*, **151**: 795–808.
- Cochran, J. R., 1986. Variations in subsidence rates along intermediate and fast spreading mid-ocean ridges. *Geophys. J. R. Astron. Soc.*, **87**: 421–454.
- Conder, J. A., D. W. Forsyth, and E. M. Parmentier, 2002. Asthenospheric flow and asymmetry of the East Pacific Rise, MELT area. *J. Geophys. Res.*, **107** (B12): 2344, doi: 10.1029/2001JB000807.
- DeMets, C., R. G. Gordon, D. F. Argus, and S. Stein, 1990. Current plate motions. *Geophys. J. Int.*, **101**: 425–478.
- Dogliani, C., E. Carminati, and E. Bonatti, 2003. Rift asymmetry and continental uplift. *Tectonics*, **22** (3): 1024, doi: 10.1029/2002TC001459.
- Eberle, M. A., and D. W. Forsyth, 1998. Evidence from the asymmetry of fast-spreading ridges that the axial topographic high is due to extensional stresses. *Nature*, **394**: 360–363.
- Forsyth, D. W., S. C. Webb, L. M. Dorman, and Y. Shen, 1998. Phase velocities of Rayleigh waves in the MELT experiment on the East Pacific Rise. *Science*, **280**: 1235–1238.
- Gao, S. S., P. M. Davis, K. H. Liu, P. D. Slack, Y. A. Zorin, *et al.*, 1994. Seismic anisotropy and mantle flow beneath the Baikal rift zone. *Nature*, **371**: 149–151.
- Grand, S. P., van der R. D. Hilst, and S. Widiyantoro, 1997. Global seismic topography: a snapshot of convection in the Earth. *GSA Today*, **7**: 1–7.
- Hess, H. H., 1962. History of ocean basins. In: *Petrologic Studies; A Volume to Honor A. F. Buddington*. A. E. J. Engel, *et al.*, eds., Geological Society of America, New York, 599–620.
- Holmes, A., 1931. Radioactivity and earth movements. *Trans. Geol. Soc., Glasgow*, **18**: 559–606.
- Kane, K. A., and D. E. Hayes, 1992. Tectonic corridors in the South Atlantic: Evidence for long-lived mid-ocean ridge segmentation. *J. Geophys. Res.*, **97**: 17317–17330.
- King, S. D., and J. Ritsema, 2000. African hotspot volcanism: small-scale convection in the upper mantle beneath cratons. *Science*, **290**: 1137–1140.
- Marty, J. C., and A. Cazenave, 1989. Regional variations in subsidence rate of oceanic plates; a global analysis. *Earth Planet. Sci. Lett.*, **94**: 301–315.
- Muller, R. D., W. R. Roest, J. Y. Royer, L. M. Gahagan, and J. G. Sclater, 1997. Digital isochrones of the world's ocean floor. *J. Geophys. Res.*, **102**(B2): 3211–3214.
- Oxburgh, E. R., and E. M. Parmentier, 1977. Compositional and density stratification in oceanic lithosphere: Causes and consequences. *J. Geol. Soc. London*, **133**: 343–355.
- Parsons, B., and J. G. Sclater, 1977. An analysis of the variation of ocean floor bathymetry and heat flow with age. *J. Geophys. Res.*, **82**(B5): 803–827.
- Phipps Morgan, J., and W. H. F. Smith, 1992. Flattening of the seafloor depth-age curve as a response to asthenospheric flow. *Nature*, **359**: 524–527.
- Silver, P. G., and W. E. Holt, 2002. The mantle flow field beneath western North America. *Science*, **295**: 1054–1057.
- Smith, W. H. F., and D. T. Sandwell, 1997. Global seafloor topography from satellite altimetry and ship depth soundings. *Science*, **277**: 1957–1962.
- Turcotte, D. L., and G. Schubert, 2002. *Geodynamics*. 2nd edition. Cambridge Univ. Press, Cambridge, 456pp.
- Wessel, P., and W. H. F. Smith, 1995. New version of the Generic mapping Tools released. *Eos Trans AGU*, **76**: 329.